Chapter 11
Analytical and Numerical Methods for Analysis of Stress Singularity in Three-Dimensional Problems of Elasticity Theory

Valerii P. Matveenko, Andrey Yu. Fedorov, Tatiana O. Korepanova, Natalja V. Sevodina, and Igor N. Shardakov

Abstract Different variants of stress singularity analysis in three-dimensional problems of elasticity theory are considered. A complete system of eigensolutions is developed for different variants of circular conical bodies: solid cone, hollow cone, a composite cone under different variants of boundary conditions on the lateral surfaces. The applicability of the constructed eigensolutions for estimating the character of stress singularity at the vertices of conical bodies is considered. The numerical results presented in the study provide insight into the character of stress singularity at the vertices of solid and hollow cones under different variants of boundary conditions on the lateral surfaces. A method for constructing singular solutions for conical bodies is suggested and variants of its numerical realization based on the finite element method are considered. The results of conducted numerical experiments demonstrate the efficiency and reliability of the proposed method. The computation of eigenvalues allows us to determine the character of stress singularity in homogeneous and composite, circular and non-circular cones under different boundary conditions. The work presents an algorithm for the finite-element analysis of singular solutions to three-dimensional problems of elasticity theory for elastic bodies of isotropic, anisotropic, and functionally graded materials. The algorithm is based on determination of a power law relationship for stresses in the vicinity of singular points. The algorithm was verified by solving two- and three-dimensional problems and comparing the obtained results with those available in the literature.

Key words: Singular points, 2D and 3D problems of elasticity theory, Stress singularity, Closed-form solution, Numerical solutions, Finite element method

Valerii P. Matveenko · Andrey Yu. Fedorov · Tatiana O. Korepanova · Natalja V. Sevodina · Igor N. Shardakov
Institute of Continuous Media Mechanics of the Ural Branch of RAS, 614018, Academician Korolev Street, 1, Perm, Russian Federation,
e-mail: mvp@icmm.ru,fedorov@icmm.ru,ton@icmm.ru,natsev@icmm.ru,shardakov@icmm.ru

H. Altenbach et al. (eds.), *Advances in Solid and Fracture Mechanics*,
Advanced Structured Materials 180,
https://doi.org/10.1007/978-3-031-18393-5_11

11.1 Introduction

One of the important results of classical elasticity theory is that it provides the existence of singular solutions associated with the occurrence of infinite stresses at points (called singular) where smoothness of the body surface is violated, the type of boundary conditions is changed, or contact of different materials takes place, as well as inside the body, at points where the condition for smoothness of the interface between different materials is violated. An example of theoretical justification of the concept that the existence of singular solutions is possible under certain conditions can be found in work [12], where it is shown that in the vicinity of angular points the equations of linear elasticity theory have a solution in the following form

$$\sigma \sim \sum_{n=1} K_n f_n r^{\lambda_n - 1}, \quad r \to 0, \quad c < \mathrm{Re}\lambda_1 < \mathrm{Re}\lambda_2 < \ldots < \mathrm{Re}\lambda_n < \ldots, \qquad (11.1)$$

or a more complex solution with logarithmic components in the case of multiple points of the spectrum λ_n. Here, r is the distance to the angular point, K_n are constants (called the stress intensity coefficients); f_n are the functions of angular distribution of the stress field σ in the vicinity of the angular point, which in the planar case depend on a single polar angular variable φ at $c = 0$, whereas in the spatial case — on two spherical coordinates φ, θ at $c = -0.5$. The form of solution (11.1) suggests that if there are λ_n, satisfying the condition $\mathrm{Re}\,\lambda_\mathrm{n} < 1$, the stresses tend to infinity at r tending to zero.

Singular points of different types are often found in computational models constructed for solving various applied problems of the theory of elasticity. The existence of singular solutions suggests that in general the vicinities of singular points are the zones of strong stress concentration that triggers the fracture process in a body. The stress behavior in the vicinity of singular points has long been the focus of many studies. For two- and three-dimensional problems of linear elasticity theory, different variants of singular points have been considered. The results obtained in this field are presented in sufficient detail in review papers [5, 25, 28, 31, 32]. Among the variety of problems with singular points, one of the first and most studied is the problem for the crack tip, which is one of the main objects of study in fracture mechanics. The distinguishing features of problems in fracture mechanics for bodies with acute-angle notches are specified in works by N. F. Morozov [21, 22]: the stress field in the vicinity of a angular notch consists of regular and singular components, and the singularity exponent depends on the opening angle of the notch.

One of the approaches to the construction of solutions of the form (11.1) is based on studying singular regions. In two-dimensional problems, the objects of investigation are the neighborhoods of vertices of wedge-shaped regions: homogeneous or composite plane wedges with boundary conditions specified on their faces (in terms of stresses or displacements). Over a more than half-century history of studies on this topic almost all possible variants of wedge-shaped bodies have been considered: homogeneous and composite, isotropic and anisotropic, functionally gradient [7, 8], etc. For three-dimensional problems, two classes of regions can be distinguished: vicinities of points on the edge of a spatial wedge and vicinities of vertices of homogeneous and composite conical regions, such as vertices of circular and non-circular cones, triangular and polyhedral wedges. Here it should be noted that mechanical characteristics of such regions may correspond to those of isotropic, anisotropic, and even functionally graded materials. Interest in three-dimensional problems of the first class has considerably diminished due to the results of some works, including [9, 20], where it is shown that solutions to the plane and antiplane problems for wedges located in the planes perpendicular to the edge of a spatial wedge determine the type of stress singularity at the points of the edge through which the corresponding plane passes.

In the last few decades, the number of works devoted to the study of stress singularity at the vertex of a polyhedral wedge and a cone has considerably increased. Most of these problems were solved using different variants of numerical methods, mainly finite and boundary element methods. Among the works using the ideas of various numerical methods worthy of note are the studies, which are based on the finite element method [1, 6, 13, 16, 19, 23, 24], on the boundary element method [11, 30], and on the application of the Mellin transformation to initial two-dimensional boundary integral equations [2]. In [16], a numerical method was developed to estimate the nature of the stress singularity at the vertex of a cone with elliptic base and homogeneous boundary conditions. In continuation to these studies, [19] presents a series of numerical methods, which makes it possible to obtain new results for different variants of cones, in particular, for homogeneous and composite, circular and non-circular cones under homogeneous and mixed boundary conditions.

As in other sections of the theory of elasticity, the analytical methods play an important role in the construction of singular solutions, and are still considered as an effective instrument both for obtaining specific numerical results and testing numerical methods. In three-dimensional problems, analytical methods are mainly applied to circular cones (axisymmetric conical regions: homogeneous [3, 14, 15, 33] and composite [14, 26, 27]). One of the first examples of analytical treatment of these problems is [3], which considers a solid cone under axisymmetric deformation and rotation with boundary conditions specified in terms of displacements and stresses. In further studies, the analytical solutions of some particular problems were obtained. For example, works [26, 27] present the results for a composite cone under axisymmetric deformation. In this case, a composite cone is a structure consisting of two nested cones, which have a common contact area. The solutions were obtained for ideal contact and ideal sliding conditions. In [33], an axisymmetric problem for a circular cone of transversally isotropic material is considered. A fairly complete review of works dealing with the study of circular cones by analytical methods is given in [32]. Among the cited works, [15] is the most comprehensive study on the subject. Here, an analytical solution for a solid circular cone was constructed and numerical results, disclosing the nature of the stress singularity at the vertex of a solid circular cone with the stress and displacement boundary conditions on the lateral surface, were obtained. In [14], a full spectrum of analytical eigenvalues for different variants of cones (solid, hollow, composite) is specified and evaluation of stress singularity exponents for solid and hollow cones under different boundary conditions on the lateral surfaces is illustrated by some numerical simulations.

11.2 Analysis of Stress Singularity Based on the Constructed Analytical Eigensolutions for Semi-infinite Circular Conical Bodies

Let us consider a homogeneous circular cone (Fig. 11.1a) whose vertex coincides with the center of spherical coordinates r, θ, φ and its base is perpendicular to the axis $\theta = 0$. The cone occupies a volume $0 \leq r < \infty$, $\theta_1 \leq \theta \leq \theta_0$, $0 \leq \varphi \leq 2\pi$, and its boundary is defined by coordinate surfaces $\theta = \theta_1$, $\theta = \theta_0$. The variant corresponds to a solid cone.

We need to construct eigensolutions satisfying the homogeneous equilibrium equations

$$(1+S)\,\mathrm{grad}\,\mathrm{div}\mathbf{U} - \mathrm{rot}\,\mathrm{rot}\mathbf{U} = 0 \tag{11.2}$$

and one of the homogeneous boundary conditions on the surfaces $\theta = \theta_1$, $\theta = \theta_0$ for displacements

$$u_r = 0,\ \ u_\theta = 0,\ \ u_\varphi = 0, \tag{11.3}$$

and stresses

$$\sigma_{r\theta} = 0,\ \ \sigma_{\theta\theta} = 0,\ \ \sigma_{\theta\varphi} = 0, \tag{11.4}$$

or mixed boundary conditions, which in terms of mechanics, correspond to ideal sliding on the lateral surface

$$u_\theta = 0,\ \ \sigma_{r\theta} = 0,\ \ \sigma_{\theta\varphi} = 0. \tag{11.5}$$

For the examined body of rotation and boundary conditions (11.3)–(11.5), the eigen solutions can be represented as a Fourier series in the circular coordinate φ

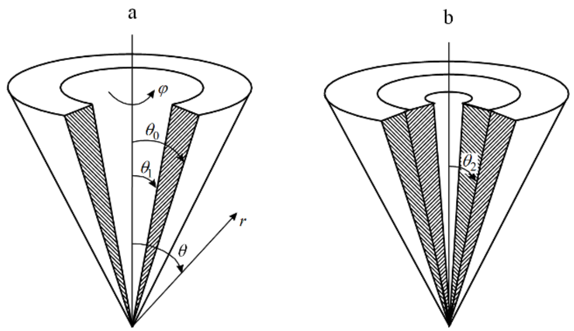

Fig. 11.1 Variants of conical bodies: hollow cone (a); hollow composite cone (b)

$$
\begin{aligned}
u_r(r,\theta,\varphi) &= u_0(\theta)\, r^{\alpha} + \sum_{k=1}^{\infty} [u_k(\theta)\, r^{\alpha} \sin(k\varphi)], \\
u_\theta(r,\theta,\varphi) &= \mathrm{v}_0(\theta)\, r^{\alpha} + \sum_{k=1}^{\infty} [\mathrm{v}_k(\theta)\, r^{\alpha} \sin(k\varphi)], \\
u_\varphi(r,\theta,\varphi) &= w_0(\theta)\, r^{\alpha} + \sum_{k=1}^{\infty} [w_k(\theta)\, r^{\alpha} \cos(k\varphi)].
\end{aligned}
\tag{11.6}
$$

Here, the dependence on the radius is represented according to (11.1) $S = 1/(1-2\nu)$; ν is Poisson's ratio; $\mathbf{U}$ is the displacement vector, u_r, u_θ, u_φ are the components of the vector of displacements along the axes r, θ, φ; $\sigma_{r\theta}$, $\sigma_{\theta\theta}$, $\sigma_{\theta\varphi}$ are the components of the stress tensor, α is the characteristic exponent.

If $\theta_1 = 0$, then the examined region is bounded by only one coordinate surface $\theta = \theta_0$, and at $\theta = 0$ the regularity conditions must be satisfied

$$
\partial u_r/\partial\theta = 0, \quad u_\theta = 0, \quad u_\varphi = 0. \tag{11.7}
$$

Within the framework of the suggested problem formulation we can also consider a composite cone occupying the domain $V = V^{(1)} + V^{(2)}$, where the subdomain $V^{(1)}$ (subdomain $V^{(2)}$) represents the cone segment made of the material with shear modulus $\mu^{(1)}$ ($\mu^{(2)}$) and Poisson's ratio $\nu^{(1)}$ ($\nu^{(2)}$) and its geometry is determined by the relations $0 \le r \le \infty$, $0 \le \varphi \le 2\pi$, $\theta_2 \le \theta \le \theta_0$ ($\theta_1 \le \theta \le \theta_2$). In particular cases, θ_1 and θ_0 can be equal to 0 and π, respectively.

For a composite cone (Fig. 11.1b), the eigensolutions (11.6) are constructed for each of the subdomains, and at the contact boundary $\theta = \theta_2$ one can set ideal bonding conditions

$$
\begin{aligned}
u_r^{(1)} &= u_r^{(2)}, \quad & u_\varphi^{(1)} &= u_\varphi^{(2)}, \quad & u_\theta^{(1)} &= u_\theta^{(2)}, \\
\sigma_\theta^{(1)} &= \sigma_\theta^{(2)}, \quad & \tau_{r\theta}^{(1)} &= \tau_{r\theta}^{(2)}, \quad & \tau_{\varphi\theta}^{(1)} &= \tau_{\varphi\theta}^{(2)},
\end{aligned}
\tag{11.8}
$$

or ideal sliding conditions

$$
u_\theta^{(1)} = u_\theta^{(2)}, \quad \sigma_\theta^{(1)} = \sigma_\theta^{(2)}, \quad \tau_{r\theta}^{(1)} = \tau_{r\theta}^{(2)} = \tau_{\varphi\theta}^{(1)} = \tau_{\varphi\theta}^{(2)} = 0. \tag{11.9}
$$

After substituting equations (11.6) into equilibrium equations (11.2) and changing to a new independent variable $x = (1-\cos\theta)/2$, we obtain for each of the harmonics of the Fourier series the following equations:

$$
\begin{aligned}
&x(1-x)\frac{d^2 u_k(x)}{dx^2} + (1-2x)\frac{du_k(x)}{dx} + \frac{\left[4xR_1(x-1)+k^2\right]}{4x(x-1)} u_k(x) + \\
&+\frac{x(1-x)R_2}{\sqrt{x(1-x)}}\frac{d\mathrm{v}_k(x)}{dx} + \frac{R_2}{\sqrt{x(1-x)}}\left[\left(\frac{1}{2}-x\right)\mathrm{v}_k(x) - \frac{kw_k(x)}{2}\right] = 0,
\end{aligned}
\tag{11.10a}
$$

$$G_1x(1-x)\frac{d^2v_k(x)}{dx^2}+G_1(1-2x)\frac{dv_k(x)}{dx}+\frac{\left[4xG_2(x-1)+k^2+G_1\right]}{4x(x-1)}v_k(x)+$$
$$+G_3\sqrt{x(1-x)}\frac{d}{dx}u_k(x)+\left[\frac{k(1-G_1)}{2}\frac{dw_k(x)}{dx}+\frac{(G_1+1)k(2x-1)}{4x(x-1)}w_k(x)\right]=0, \tag{11.10b}$$

$$x(1-x)\frac{d^2w_k(x)}{dx^2}+(1-2x)\frac{dw_k(x)}{dx}+\frac{\left[4xG_2(x-1)+G_1k^2+1\right]}{4x(x-1)}w_k(x)+$$
$$+\frac{kG_3}{2\sqrt{x(1-x)}}u_k(x)+\left[\frac{(G_1-1)k}{2}\frac{dv_k(x)}{dx}+\frac{(G_1+1)k(2x-1)}{4x(x-1)}\cdot v_k(x)\right]=0. \tag{11.10c}$$

Here, the following representations are used

$$R_1=\frac{2(1-\nu)(1-\alpha)(\alpha+2)}{(2\nu-1)};\quad R_2=\frac{(3-\alpha-4\nu)}{(-1+2\nu)};$$

$$G_1=\frac{2(1-\nu)}{(1-2\nu)};\quad G_2=\alpha(1+\alpha);\quad G_3=\frac{2(\alpha+4-4\nu)}{(1-2\nu)}.$$

In view of equation (11.6), the boundary conditions (11.3)–(11.5) and the regularity condition (11.7) are transformed exactly in the same way:

$$u_k(x)=0;\qquad v_k(x)=0;\qquad \mathrm{w}_k(x)=0; \tag{11.11}$$

$$\mu\left[\sqrt{x(1-x)}\frac{du_k(x)}{dx}+(\alpha-1)v_k(x)\right]=0; \tag{11.12a}$$

$$\mu\left[(2S-\alpha+\alpha S)u_k(x)+(1+S)\sqrt{x(1-x)}\frac{dv_k(x)}{dx}+\right.$$
$$\left.+\left(\frac{1}{2}-x\right)\frac{(S-1)}{\sqrt{x(1-x)}}v_k(x)+\frac{k(1-S)}{2\sqrt{x(1-x)}}w_k(x)\right]=0; \tag{11.12b}$$

$$\mu\left[\sqrt{x(1-x)}\frac{dw_k(x)}{dx}-\frac{(1-2x)}{2\sqrt{x(1-x)}}w_k(x)+\frac{k}{2\sqrt{x(1-x)}}v_k(x)\right]=0; \tag{11.12c}$$

$$\sqrt{x(1-x)}\frac{du_k(x)}{dx}=0;\qquad v_k(x)=0;\qquad \mathrm{w}_k(x)=0. \tag{11.13}$$

The variant for the zero harmonic of the Fourier series is considered separately, since it does not explicitly follow from the algorithm for constructing partial solutions of the system of differential equations (11.10) for any value of $k\neq 0$. At $k=0$ there are two problems: axisymmetric rotation and axisymmetric deformation. In the first problem, the component of the displacement vector w_0 is determined by equation (11.10c). In the axisymmetric deformation problem, the displacement vector components u_0, v_0 are defined by equations (11.10a), (11.10b).

Solutions for the function w_0 are derived in the form of a generalized power series

$$w_0(x) = \sum_{m=0}^{\infty} \left[A_m x^{(m+\beta)} \right], \tag{11.14}$$

where A_m are the coefficients of the power series; β is the characteristic exponent.

The possibility of constructing a solution in the form (11.14) is substantiated in [18]. The point $x = 0$ for equation (11.10c) is a regular singular point. In this case, one of the partial solutions is written in the form of series (11.14), for which the region of convergence is the range of the variable $0 \leq x \leq 1$, since the value $x = 1$ is a zero of the function nearest to the point $x = 0$ for a higher derivative.

To find the coefficients of the series A_m and the characteristic exponent β, equation (11.14) is substituted into (11.10c). By equating the expressions with similar powers of x to zero, we obtain the recurrence relation for A_m:

$$\begin{aligned} &(2\beta+2m+1)(2\beta+2m-1)A_m+ \\ &\quad +4\left[\alpha(\alpha+1)-(2\beta+2m-1)\ (\beta+m-1)\right]A_{m-1}- \\ &\quad -4(\alpha+2-m-\beta)(\alpha-1+m+\beta)A_{m-2}=0, \quad (m=0,1,2,\ldots) \end{aligned} \tag{11.15}$$

From the condition for the existence of a nonzero solution with respect to A_0 we get the characteristic equation

$$(2\beta+1)(2\beta-1) = 0, \tag{11.16}$$

where $\beta_1 = 0.5$ and $\beta_1 = -0.5$ are its roots.

According to the theory of ordinary differential equations [18], there is always a solution in the form of a generalized power series (11.14) that corresponds to the largest root β_1. Substituting the value of root β_1 into (11.15), we obtain a recurrence relation for $A_m^{(1)}$:

$$A_m^{(1)} = \frac{\left(2m^2-\alpha-\alpha^2-m\right)}{m(1+m)} A_{m-1}^{(1)} + \frac{(2\alpha-1+2m)(2\alpha+3-2m)}{4m(1+m)} A_{m-2}^{(1)}, \quad (m>0,\ A_0^{(1)}=1). \tag{11.17}$$

Here and hereafter, the upper index defines the number of the partial solution.

The transformations performed allow us to obtain the first partial solution, which has the form of a generalized power series for equation (11.10c):

$$w_0^{(1)}(x) = \sum_{m=0}^{\infty} \left[A_m^{(1)} x^{\left(m+\frac{1}{2}\right)} \right]. \tag{11.18}$$

The difference in roots of the characteristic equation [10], i.e. $\gamma = \beta_1 - \beta_2$, is crucial for constructing a second linearly independent partial solution in the form of a generalized power series. If γ is not a positive integer, there exists a second linearly independent solution in the form of a generalized power series (11.14). If

γ is a positive integer, then in the general case the existence of a second partial solution in the form of generalized power series (11.14) is not guaranteed.

To exclude this uncertainty, we applied an approach, which is based on a sequential reduction of the original differential equation by making use of the first partial solution and keeping a fixed number of terms in the series. A series segment for the second partial solution of the original differential equation is obtained as follows. After reduction, the resulting series segment is integrated and the result of the integration is multiplied by the generalized power series corresponding to the first partial solution. The form of the obtained series segment for the second partial solution determines the characteristic exponent of the generalized power series and the terms including the logarithmic functions. It should be noted that partial solutions subsequent to the second partial solution [10] include the logarithmic functions of higher degree (compared to the first function).

Thus, the proposed method makes it possible to successively determine the types of generalized power series of all partial solutions of the original differential equation and to single out from all partial solutions the regular and irregular ones, in our case, at value $x = 0$. These capabilities of the method hold much promise for constructing solutions to particular problems, for example, that of a hollow cone.

Using the proposed method, a second partial solution $\omega_0^{(2)}$ is obtained :

$$\omega_0^{(2)}(x) = \sum_{m=0}^{\infty} \left\{ \left[A_m^{(2)} + B_m^{(2)} \cdot \ln(x) \right] x^{(m-1/2)} \right\}, \tag{11.19}$$

where the coefficients $A_m^{(2)}$, $B_m^{(2)}$ are determined from the recurrence relations

$$\begin{aligned} B_m^{(2)} &= \frac{\left[(m-1)(2m-3)-\alpha^2-\alpha\right]}{m(m-1)} B_{m-1}^{(2)} - \frac{(2m-3+2\alpha)(2m-5-2\alpha)}{4m(m-1)} B_{m-2}^{(2)}, \\ A_m^{(2)} &= \frac{(1-2m)}{m(m-1)} B_m^2 + \frac{\left[(m-1)(2m-3)-\alpha^2-\alpha\right]}{m(m-1)} A_{m-1}^{(2)} + \frac{(4m-5)}{m(m-1)} B_{m-1}^{(2)} - \\ &\quad - \frac{(2m-3+2\alpha)(2m-5-2\alpha)}{4m(m-1)} A_{m-2}^{(2)} - \frac{2(m-2)}{m(m-1)} B_{m-2}^{(2)}. \end{aligned} \tag{11.20}$$

From the form of the obtained solutions $w_0^{(1)}$, $w_0^{(2)}$ it follows that $w_0^{(1)}$ is a regular solution, and $w_0^{(2)}$ is an irregular solution at $x = 0$.

The general solution of the differential equation (11.10c) can be written as

$$w_0(x) = C_1 \cdot w_0{}^{(1)}(x) + C_2 \cdot w_0{}^{(2)}(x), \tag{11.21}$$

where C_1, C_2 are the constants determined from a preset combination of boundary conditions (11.3)–(11.5). To construct partial solutions to equations (11.10a) and (11.10b) corresponding to the axisymmetric deformation variant, we solve this system for v_0 [18]:

$$
\begin{gathered}
v_0(x)=\frac{\sqrt{x(1-x)}}{(1-\alpha)S+2}\times\\
\times\left\{\frac{(S+1)}{\left(\alpha+\alpha^2\right)}\left[\left(x^2-x\right)\frac{d^3u_0(x)}{dx^3}+(4x-2)\frac{d^2u_0(x)}{dx^2}\right]-(2S+1)\frac{du_0(x)}{dx}\right\}
\end{gathered}
\tag{11.22}
$$

and obtain for the function u_0 the fourth-order differential equation.

$$
\begin{gathered}
x^2(x-1)^2\frac{d^4u_0(x)}{dx^4}-x(x-1)(4-8x)\frac{d^3u_0(x)}{dx^3}+\\
+\left[2-2x(\alpha+3)(\alpha-2)(-1+x)\right]\frac{d^2u_0(x)}{dx^2}-\\
-\alpha(2+2\alpha)(2x-1)\frac{du_0(x)}{dx}-\left(\alpha+\alpha^2\right)(1-\alpha)(2+\alpha)u_0(x)=0.
\end{gathered}
\tag{11.23}
$$

This equation is a differential equation with a regular singular point, so that linearly independent partial solutions can be represented in the form of convergent generalized power series. Using the above approach for constructing such series, we obtain four partial solutions $u_0^{(1)}$, $u_0^{(2)}$, $u_0^{(3)}$, $u_0^{(4)}$ in the following form:

$$
\begin{aligned}
u_0^{(1)}(x)&=\sum_{m=0}^{\infty}\left[A_m^{(1)}x^{(m+1)}\right];\\
u_0^{(2)}(x)&=\sum_{m=0}^{\infty}\left[A_m^{(2)}x^{m}\right];\\
u_0^{(3)}(x)&=\sum_{m=0}^{\infty}\left\{\left[A_m^{(3)}+B_m^{(3)}\ln(x)\right]x^{(m+1)}\right\}\\
u_0^{(4)}(x)&=\sum_{m=0}^{\infty}\left\{\left[A_m^{(4)}+B_m^{(4)}\ln(x)\right]x^{m}\right\},
\end{aligned}
\tag{11.24}
$$

where the coefficients $A_m^{(1)}$, $A_m^{(2)}$, $A_m^{(3)}$, $A_m^{(4)}$, $B_m^{(3)}$, $B_m^{(4)}$, are determined from the recurrence relations available on https://www.icmm.ru/compcoeff/.

Substituting (11.24) into expression (11.22), we obtain partial solutions $v_0^{(1)}$, $v_0^{(2)}$, $v_0^{(3)}$, $v_0^{(4)}$ for the function v_0:

$$
\begin{aligned}
v_0^{(1)}(x)&=\frac{\sqrt{x(1-x)}}{[(\alpha-1)S-2]\left(\alpha+\alpha^2\right)}\sum_{m=0}^{\infty}\left[P_m^{(1)}x^m\right],\\
v_0^{(2)}(x)&=\frac{\sqrt{x(1-x)}}{[(\alpha-1)S-2]\left(\alpha+\alpha^2\right)}\sum_{m=0}^{\infty}\left[P_m^{(2)}x^m\right],\\
v_0^{(3)}(x)&=\frac{\sqrt{x(1-x)}}{[(\alpha-1)S-2]\left(\alpha+\alpha^2\right)}\left\{\frac{(1+S)}{x}+\sum_{m=0}^{\infty}\left[\left(P_m^{(3)}+D_m^{(3)}\ln(x)\right)x^m\right]\right\},\\
v_0^{(4)}(x)&=\frac{\sqrt{x(1-x)}}{[(\alpha-1)S-2]\left(\alpha+\alpha^2\right)}\left\{\sum_{m=0}^{\infty}\left[\left(P_m^{(4)}+D_m^{(4)}\cdot\ln(x)\right)x^{(m-1)}\right]\right\},
\end{aligned}
\tag{11.25}
$$

where the coefficients $P_m^{(1)}$, $P_m^{(2)}$, $P_m^{(3)}$, $P_m^{(4)}$, $D_m^{(3)}$, $D_m^{(4)}$ are determined by the expressions posted on https://www.icmm.ru/compcoeff/.

The general solution for u_0 and v_0 are as follows:

$$\begin{aligned} u_0(x) &= C_1 \cdot u_0^{(1)}(x) + C_2 \cdot u_0^{(2)}(x) + C_3 \cdot u_0^{(3)}(x) + C_4 \cdot u_0^{(4)}(x), \\ v_0(x) &= C_1 \cdot v_0^{(1)}(x) + C_2 \cdot v_0^{(2)}(x) + C_3 \cdot v_0^{(3)}(x) + C_4 \cdot v_0^{(4)}(x), \end{aligned} \tag{11.26}$$

where C_1, C_2, C_3, C_4 are the constants determined from a preset combination of boundary conditions (11.3)–(11.5).

To construct partial solutions to the system of equations (11.10), we perform a series of transformations [18], and obtain, as a result, a system of two differential equations with respect to w_k, v_l:

$$\begin{aligned} & f_4(x)\frac{d^4 w_k(x)}{dx^4} + f_3(x)\frac{d^3 w_k(x)}{dx^3} + f_2(x)\frac{d^2 w_k(x)}{dx^2} + \\ & \qquad + f_1(x)\frac{d w_k(x)}{dx} + f_0(x)\, w_k(x) = 0, \end{aligned} \tag{11.27a}$$

$$\begin{aligned} & \psi_2(x)\frac{d^2 v_k(x)}{dx^2} + \psi_0(x)\, v_k(x) = \phi_3(x)\frac{d^3 w_k(x)}{dx^3} + \\ & \qquad + \phi_2(x)\frac{d^2 w_k(x)}{dx^2} + \phi_1(x)\frac{d w_k(x)}{dx} + \phi_0(x)\, w_k(x), \end{aligned} \tag{11.27b}$$

where $f_0, f_1, f_2, f_3, f_4, \psi_0, \psi_2, \phi_0, \phi_1, \phi_2, \phi_3$ are written as:

$$\begin{aligned} f_0(x) &= \frac{1}{2}x\alpha(\alpha+1)(x-1)\left[2x(\alpha+3)(\alpha-2)(x-1)+k^2-1\right] + \\ &+ \frac{1}{16}(k-1)^2(k+1)^2, \\ f_1(x) &= x(1-x)(2x-1)\left[4x\left(\alpha^2+\alpha-3\right)(x-1)+\frac{1}{2}k^2-\frac{1}{2}\right], \\ f_2(x) &= -\frac{1}{2}x^2(x-1)^2\left[4x\left(\alpha^2+\alpha-18\right)(x-1)+\frac{1}{2}k^2-13\right], \\ f_3(x) &= 6x^3(x-1)^3(2x-1), \\ f_4(x) &= x^4(x-1)^4, \\ \psi_0(x) &= x\alpha(\alpha+1)(x-1)+\frac{1}{4}(1-k^2), \\ \psi_2(x) &= x^2(x-1)^2, \\ \phi_0(x) &= -\frac{1}{2}x\left[4x\alpha(\alpha+1)(x-1)-k^2+1\right]\frac{(2x-1)}{k}, \\ \phi_1(x) &= \frac{1}{2}x\left[4x\left(\alpha^2+\alpha-4\right)(x-1)-k^2+1\right]\frac{(x-1)}{k}, \\ \phi_2(x) &= -5x^2(2x-1)\frac{(x-1)^2}{k}, \\ \phi_3(x) &= 2x^3\frac{(x-1)^3}{k}. \end{aligned} \tag{11.28}$$

Furthermore, the performed transformations results in the relation that establishes the dependence of the function u_k on the functions w_k, v_k and their derivatives:

$$u_k(x) = \frac{\sqrt{x(1-x)}}{2x(x-1)k(S\alpha+2S+2)}\left\{4x^2(x-1)\frac{d^2w_k(x)}{dx^2}+4x(2x-1)\frac{dw_k(x)}{dx}- \right.$$
$$- \left[4\alpha x(x-1)(1+\alpha)+k^2(S+1)+1\right]\cdot w_k(x)-$$
$$\left. - \left[2kSx(x-1)\frac{dv_k(x)}{dx}+k(2x-1)(S+2)v_k(x)\right]\right\}. \tag{11.29}$$

Equation (11.27a) is independent of equation (11.27b) and is a fourth-order linear differential equation with respect to the function w_k. Equation (11.27b) can be considered as a second-order differential equation with respect to v_k with the right-hand side depending on w_k. This specific feature of differential equations (11.27) and the resulting relation (11.29) allow us to define a sequence of partial solutions for the functions ω_k, v_k, u_k. The concept of this sequence is as follows. At the first stage, from the solution of equation (11.27a) we get four partial solutions $w_k^{(1)}, w_k^{(2)}, w_k^{(3)}, w_k^{(4)}$ written in the following form

$$\omega_k^{(1)}(x) = \sum_{m=0}^{\infty}\left[A_m^{(1)}x^{\left(m+\frac{k+1}{2}\right)}\right], \qquad \omega_k^{(2)}(x) = \sum_{m=0}^{\infty}\left[A_m^{(2)}x^{\left(m+\frac{k-1}{2}\right)}\right],$$
$$\omega_k^{(3)}(x) = \sum_{m=0}^{\infty}\left[\left(A_m^{(3)}+B_m^{(3)}\ln(x)\right)x^{\left(m-\frac{k-1}{2}\right)}\right], \tag{11.30}$$
$$\omega_k^{(4)}(x) = \sum_{m=0}^{\infty}\left[\left(A_m^{(4)}+B_m^{(4)}\ln(x)\right)x^{\left(m-\frac{k+1}{2}\right)}\right],$$

where the coefficients $A_m^{(1)}, A_m^{(2)}, A_m^{(3)}, A_m^{(4)}, B_m^{(3)}, B_m^{(4)}$ are determined by the relations posted on https://www.icmm.ru/compcoeff/.

Sequentially substituting the obtained partial solutions into the right-hand side of equation (11.27b) and solving it as the inhomogeneous equation, we find four partial solutions $v_k^{(1)}$, $v_k^{(2)}$, $v_k^{(3)}$, $v_k^{(4)}$ written as

$$v_k^{(1)}(x) = \sum_{m=0}^{\infty}\left[P_m^{(1)}x^{\left(m+\frac{k+1}{2}\right)}\right],$$
$$v_k^{(2)}(x) = \sum_{m=0}^{\infty}\left[P_m^{(2)}x^{\left(m+\frac{k-1}{2}\right)}\right],$$
$$v_k^{(3)}(x) = \sum_{m=0}^{\infty}\left\{\left[P_m^{(3)}+D_m^{(3)}\ln(x)\right]x^{\left(m-\frac{k-1}{2}\right)}\right\}, \tag{11.31}$$
$$v_k^{(4)}(x) = \sum_{m=0}^{\infty}\left\{\left[P_m^{(4)}+D_m^{(4)}\ln(x)\right]x^{\left(m-\frac{k+1}{2}\right)}\right\},$$

where the coefficients $P_m^{(1)}, P_m^{(2)}, P_m^{(3)}, P_m^{(4)}, D_m^{(3)}, D_m^{(4)}$ are determined by the relations available on https://www.icmm.ru/compcoeff/.

Then, solving equation (11.27b) as a homogeneous one, we find two more partial solutions $v_k^{(5)}$, $v_k^{(6)}$. The form of this differential equation indicates that the point $x = 0$ is a regular singular point. The construction of partial solutions in the form of generalized power series is accomplished in the framework of the above approach. These partial solutions are written as

$$
\begin{aligned}
v_k^{(5)}(x) &= \sum_{m=0}^{\infty}\left[P_m^{(5)} x^{\left(m+\frac{k+1}{2}\right)}\right],\\
v_k^{(6)}(x) &= \sum_{m=0}^{\infty}\left[\left(P_m^{(6)} + D_m^{(6)}\ln(x)\right) x^{\left(m+\frac{k-1}{2}\right)}\right],
\end{aligned}
\tag{11.32}
$$

where $P_m^{(5)}, P_m^{(6)}, D_m^{(6)}$ are defined on https://www.icmm.ru/compcoeff/.

Then, using partial solutions $w_k^{(1)}, w_k^{(2)}, w_k^{(3)}, w_k^{(4)}$, $v_k^{(1)}, v_k^{(2)}, v_k^{(3)}$, $v_k^{(4)}$, $v_k^{(5)}$, $v_k^{(6)}$, and the obtained relation (30), we determine six partial solutions $u_k^{(1)}$, $u_k^{(2)}$, $u_k^{(3)}$, $u_k^{(4)}$, $u_k^{(5)}$, $u_k^{(6)}$, represented as

$$
\begin{aligned}
u_k^{(1)} &= \frac{2\sqrt{x(1-x)}}{kx(x-1)(S(\alpha+2)+2)} \sum_{m=0}^{\infty}\left[E_m^{(1)} x^{\left(m+\frac{k+1}{2}\right)}\right],\\
u_k^{(2)} &= \frac{2\sqrt{x(1-x)}}{kx(x-1)(S(\alpha+2)+2)} \sum_{m=0}^{\infty}\left[E_m^{(2)} x^{\left(m+\frac{k-1}{2}\right)}\right],\\
u_k^{(3)} &= \frac{2\sqrt{x(1-x)}}{kx(x-1)(S(\alpha+2)+2)} \sum_{m=0}^{\infty}\left[\left(E_m^{(3)} + G_m^{(3)}\ln(x)\right) x^{\left(m-\frac{k-1}{2}\right)}\right],\\
u_k^{(4)} &= \frac{2\sqrt{x(1-x)}}{kx(x-1)(S(\alpha+2)+2)} \sum_{m=0}^{\infty}\left[\left(E_m^{(4)} + G_m^{(4)}\ln(x)\right) x^{\left(m-\frac{k+1}{2}\right)}\right],\\
u_k^{(5)} &= \frac{\sqrt{x(1-x)}}{kx(x-1)(S(\alpha+2)+2)} \sum_{m=0}^{\infty}\left[E_m^{(5)} x^{\left(m+\frac{k+1}{2}\right)}\right],\\
u_k^{(6)} &= \frac{\sqrt{x(1-x)}}{kx(x-1)(S(\alpha+2)+2)} \sum_{m=0}^{\infty}\left[\left(E_m^{(6)} + G_m^{(6)}\ln(x)\right) x^{\left(m-\frac{k-1}{2}\right)}\right],
\end{aligned}
\tag{11.33}
$$

where the coefficients $E_m^{(1)}$, $E_m^{(2)}$, $E_m^{(3)}$, $E_m^{(4)}$, $E_m^{(5)}$, $E_m^{(6)}$, $G_m^{(3)}$, $G_m^{(4)}$, $G_m^{(6)}$ for any value of $m \geq 0$ are determined on https://www.icmm.ru/compcoeff/index2.html.

General solutions for u_k, v_k, w_k take the following form

$$
\begin{aligned}
u_k(x) &= C_1 \cdot u_k^{(1)}(x) + C_2 \cdot u_k^{(2)}(x) + C_3 \cdot u_k^{(3)}(x) +\\
&\qquad + C_4 \cdot u_k^{(4)}(x) + C_5 \cdot u_k^{(5)}(x) + C_6 \cdot u_k^{(6)}(x),\\
v_k(x) &= C_1 \cdot v_k^{(1)}(x) + C_2 \cdot v_k^{(2)}(x) + C_3 \cdot v_k^{(3)}(x) +\\
&\qquad + C_4 \cdot v_k^{(4)}(x) + C_5 \cdot v_k^{(5)}(x) + C_6 \cdot v_k^{(6)}(x),\\
w_k(x) &= C_1 \cdot w_k^{(1)}(x) + C_2 \cdot w_k^{(2)}(x) + C_3 \cdot w_k^{(3)}(x) + C_4 \cdot w_k^{(4)}(x),
\end{aligned}
\tag{11.34}
$$

where $C_1, C_2, C_3, C_4, C_5, C_6$ are the constants determined from a preset combination of boundary conditions (11.3)–(11.5).

For the examined variant of a conical body, the constructed general solutions for $k = 0$, $k \geq 1$ and the preset combination of boundary conditions are used to derive a homogeneous system of linear algebraic equations for the constants C_i. The coefficients of this system of equations depend on the vertex angles of conical bodies, elastic characteristics of materials, and the characteristic exponent α. From the condition of existence of a nonzero solution to the system of linear algebraic equations we find the exponents α, determining the nature of stress singularity at the vertices of conical bodies.

Let us consider numerical results for a solid cone ($0 \leq r \leq \infty$, $0 \leq \varphi \leq 2\pi$, $0 \leq \theta \leq \theta_0$). Here we use partial solutions, for which the regularity condition is identically fulfilled at $x = 0$ (or $\theta = 0$): $w_0^{(1)}$ is used for axisymmetric rotation; $u_0^{(1)}$, $v_0^{(1)}$, $u_0^{(2)}$, $v_0^{(2)}$ — for axisymmetric deformation without rotation; $u_k^{(1)}$, $v_k^{(1)}$, $w_k^{(1)}$, $u_k^{(2)}$, $v_k^{(2)}$, $w_k^{(2)}$, $u_k^{(5)}$, $v_k^{(5)}$ — for nonaxisymmetric deformation. All results in this work were obtained for Poisson's ratio $\nu = 0.3$. Figure 11.2 presents the values $\mathrm{Re}\,\alpha_n < 1$, determining singular solutions for a solid cone with stress and displacement boundary conditions. These values are identical to the results of [19, 15]. It should be noted that for a solid cone with stress boundary conditions, the singular solutions appear at the zero, first and second harmonics of the Fourier series, whereas for a cone with displacement boundary conditions — at the zero and first harmonics of the Fourier series. Figure 11.3 shows new results disclosing the nature of stress singularity at the vertex of a solid cone with boundary conditions of ideal sliding prescribed on its lateral surface. Here, singular solutions are possible at the zero, first and second harmonics of the Fourier series and at the angle θ_0 smaller than π.

The proposed method has proved to be effective in determining the region of singular solutions for a hollow cone with two conical boundary surfaces $\theta = \theta_0$ and

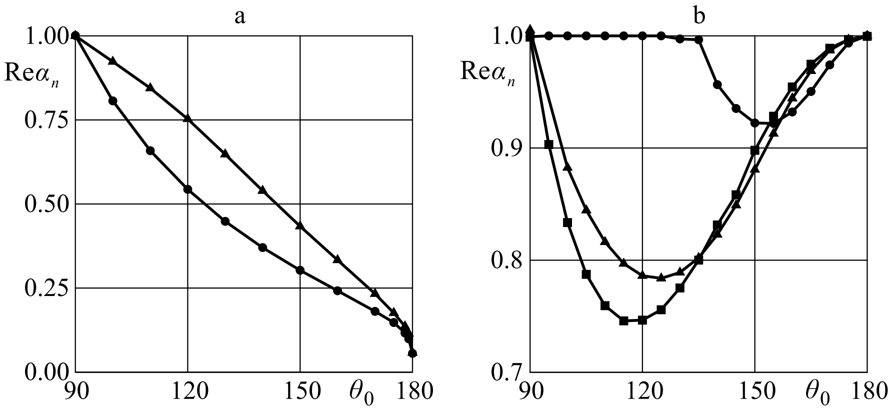

Fig. 11.2 Dependence of $\mathrm{Re}\,\alpha_n$ on the vertex angle of the solid cone with boundary conditions on the lateral surface for displacements (a) and stresses (b) (▲ — $k = 0$, • — $k = 1$, ■ — $k = 2$)

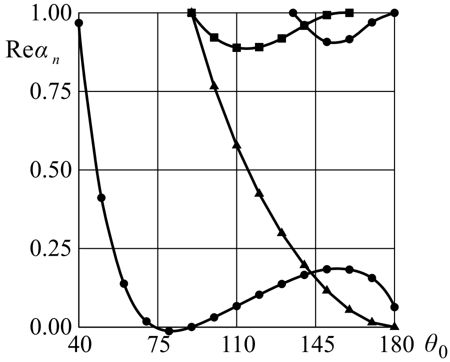

Fig. 11.3 Dependence of Reα_n on the vertex angle of the cone with boundary conditions on the lateral surface corresponding to an ideal sliding (▲ — $k = 0$, • — $k = 1$, ■ — $k = 2$)

$\theta = \theta_1$ (hollow cone) under different variants of boundary conditions. In this case, it is necessary to use all partial solutions (11.18), (11.19), (11.24), (11.25), (11.30), (11.31), (11.32) to ensure the fulfillment of boundary conditions on the two conical surfaces. As an example, Fig. 11.4 shows the dependence of eigenvalues Re$\alpha_n < 1$ on the angle of the outer conical surface θ_0 for different internal cone angles θ_1. Zero stress boundary conditions are prescribed on the conical surfaces. Here, the solid line corresponds to the actual eigenvalues and the dashed line — to the complex ones.

In the case of a hollow cone, different combinations of boundary conditions on the inner and outer conical surfaces can be used. Here we consider two variants. In the first variant, zero stresses are specified on the inner surface and zero displacements — on the outer surface. In the second variant, zero displacements are preset on the inner surface and zero stresses — on the outer surface. The variation of the stress singularity exponent Re$\alpha_n < 1$ as a function of the outer conical surface angle θ_0 at different values of the inner surface angle is shown in Fig. 11.5 for the first variant of boundary conditions. The eigenvalues, leading to the occurrence of stress singularity, appear at the values of θ_0 higher than 80°. For the second variant of the boundary conditions the dependence of eigenvalues Re$\alpha_n < 1$ is shown in Fig. 11.6.

11.3 Numerical-analytical Method of Stress Singularity Analysis at the Vertices of Circular and Non-circular Conical Bodies

We consider a semi-infinite circular or non-circular cone, whose vertex coincides with the center of spherical coordinates r, θ, φ, and the base is perpendicular to the axis $\theta = 0$. To analyze the character of the stress singularity, we need to construct eigensolutions, which will be similar in form to the asymptotic representation of solution [12],

$$u_k(r,\theta,\varphi) = r^{\lambda}\xi_k(\theta,\varphi), \qquad k = 1,2,3 \tag{11.35}$$

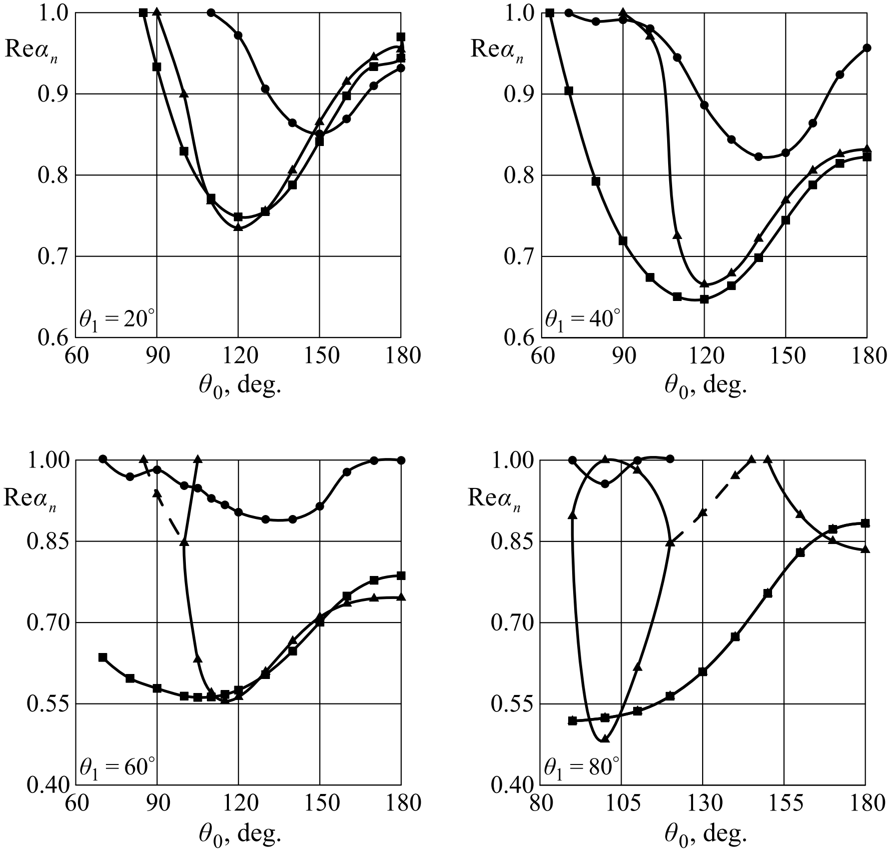

Fig. 11.4 Dependence of Reα_n on the angle θ_0 at fixed angles θ_1 of the hollow cone and zero stresses on the lateral surfaces for different values of k (▲ — $k = 0$, ● — $k = 1$, ■ — $k = 2$)

Fig. 11.5 Dependence of Reα_n on the angle θ_0 for different values of θ_1 at zero stresses on the inner surface and zero displacements on the outer lateral surface (▲ — $k = 0$, ● — $k = 1$, ■ — $k = 2$)

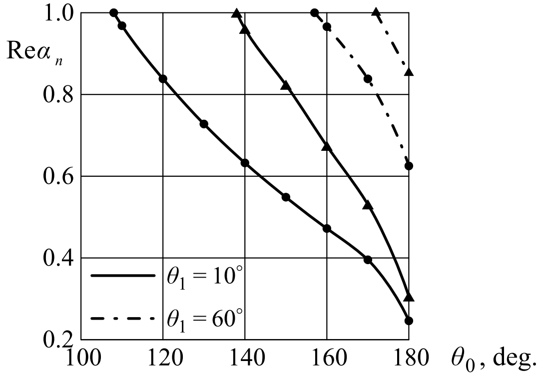

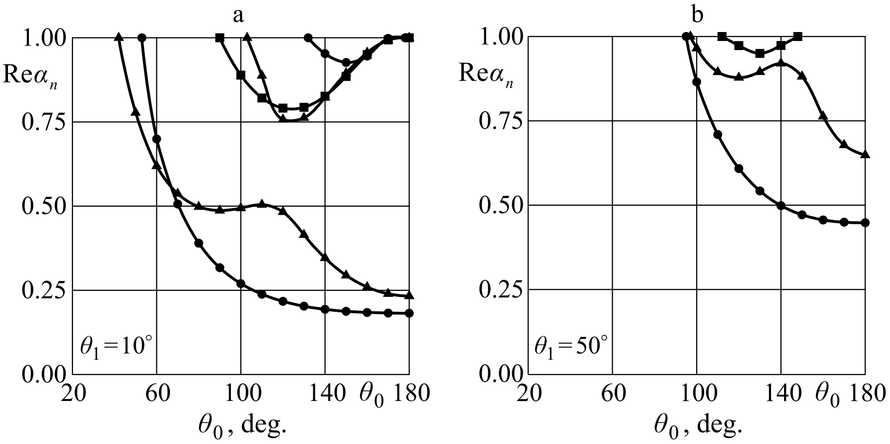

Fig. 11.6 Dependence of Reα_n on the angle θ_0 for different values of θ_1 of the hollow cone with zero displacements on the inner surface and zero stresses on the outer lateral surface (▲ — $k=0$, • — $k=1$, ■ — $k=2$)

and satisfy in the examined domain the equilibrium equations

$$\frac{1}{1-2\nu}\operatorname{grad}\operatorname{div}\mathbf{u}+\nabla^2\mathbf{u}=0 \tag{11.36}$$

and uniform boundary conditions prescribed on the lateral surface of the cone, namely, zero displacements

$$\mathbf{u}=0 \tag{11.37}$$

or zero stresses

$$\frac{\nu}{1-2\nu}\mathbf{n}\operatorname{div}\mathbf{u}+\mathbf{n}\cdot\nabla\mathbf{u}+\frac{1}{2}\mathbf{n}\times\operatorname{rot}\mathbf{u}=0. \tag{11.38}$$

Here $\mathbf{u}$ is the displacement vector, $\mathbf{n}$ is the unit vector of the external normal, ν is Poisson's ratio.

A variant of boundary conditions corresponding to the ideal sliding conditions on the lateral surface may be also of interest. These conditions are as follows:

$$u_\theta=0, \quad \tau_{r\theta}=0, \quad \tau_{\varphi\theta}=0. \tag{11.39}$$

On the lateral surface of the cone, mixed boundary conditions can be prescribed, that is, conditions (11.38) are set at $0\le\varphi\le\varphi_1$ and conditions (11.39) are specified at $\varphi_1\le\varphi\le 2\pi$.

In addition to a solid cone, the study can be conducted for a hollow cone with two lateral surfaces. For a circular cone, the domain occupied by this body is defined as follows: $0\le r\le\infty$, $0\le\varphi\le 2\pi$, $\theta_1\le\theta\le\theta_2$ ($\theta_1=0$ corresponds to a solid cone). In this case, one of the variants of boundary conditions (11.37)–(11.39) can be imposed on the lateral surfaces.

To construct eigenvalues, we substitute expressions (11.35) into Eqs. (11.36), to obtain a system of partial differential equations with respect to functions $\xi_k(\theta,\varphi)$ and parameter λ

$$\begin{aligned}
L_1(\lambda,\xi_k) &= 2(1-\nu)(k_1-2)\xi_1 + k_2(\xi_2 \operatorname{ctg}\theta + \xi_{2\theta} + \frac{1}{\sin\theta}\xi_{3\varphi}) + \\
&+ (1-2\nu)(\operatorname{ctg}\theta\,\xi_{1\theta} + \xi_{1\theta\theta} + \frac{1}{\sin^2\theta}) = 0, \\
L_2(\lambda,\xi_k) &= \left[(1-2\nu)k_1 - \frac{2(1-\nu)}{\sin^2\theta}\right]\xi_2 + k_3\xi_{1\theta} - (3-4\nu)\frac{\operatorname{ctg}\theta}{\sin\theta}\xi_{3\varphi} + \\
&+ \frac{(1-2\nu)}{\sin^2\theta}\xi_{2\varphi\varphi} + \frac{1}{\sin\theta}\xi_{3\theta\varphi} + 2(1-\nu)(\operatorname{ctg}\theta\,\xi_{2\theta} + \xi_{2\theta\theta}) = 0, \\
L_3(\lambda,\xi_k) &= (1-2\nu)(k_1 - \frac{1}{\sin^2\theta})\xi_3 + k_3\frac{1}{\sin\theta}\xi_{1\varphi} - (3-4\nu)\frac{\operatorname{ctg}\theta}{\sin\theta}\xi_{2\varphi} + \\
&+ \frac{2(1-\nu)}{\sin^2\theta}\xi_{3\varphi\varphi} + \frac{1}{\sin\theta}\xi_{2\theta\varphi} + (1-2\nu)(\operatorname{ctg}\theta\,\xi_{3\theta} + \xi_{3\theta\theta}) = 0.
\end{aligned} \tag{11.40}$$

Here, $k_1 = \lambda^2 + \lambda$, $k_2 = \lambda - 3 + 4\nu$, $k_3 = \lambda + 4 - 4\nu$, $\xi_{k\theta} = \partial\xi_k/\partial\theta$, $\xi_{k\varphi} = \partial\xi_k/\partial\varphi$, $\xi_{k\theta\theta} = \partial^2\xi_k/\partial\theta^2$, etc.

Based on the asymptotic expression (11.35), boundary conditions (11.37), (11.38) are transformed to the following form:

$$M_1(\lambda,\xi_k) \equiv \xi_1 = 0, \qquad M_2(\lambda,\xi_k) \equiv \xi_2 = 0, \qquad M_3(\lambda,\xi_k) \equiv \xi_3 = 0. \tag{11.41}$$

$$\begin{aligned}
&M_1(\lambda,\xi_k) \equiv \xi_{1\theta} + \xi_2(\lambda-1) = 0, \\
&M_2(\lambda,\xi_k) \equiv (1-\nu)\xi_{2\theta} + (1+\nu\lambda)\xi_1 + \nu \operatorname{ctg}\theta\,\xi_2 + \frac{\nu}{\sin\theta}\xi_{3\varphi} = 0, \\
&M_3(\lambda,\xi_k) \equiv \xi_{3\theta} + \frac{1}{\sin\theta}\xi_{2\varphi} - \operatorname{ctg}\theta\,\xi_3 = 0.
\end{aligned} \tag{11.42}$$

Here L_k and M_k are the differential operators.

In addition to a homogeneous cone, as an object of study we can also consider a composite cone, e.g., a circular cone occupying the domain $V = V_1 + V_2$, where the subdomain V_1 (subdomain V_2) is a segment of the cone made of the material with shear modulus G_1 (G_2) and Poisson's ratio ν_1 (ν_2). The subdomain geometry is defined by the relations $0 \le r \le \infty$, $0 \le \varphi \le 2\pi$, $\theta_1 \le \theta \le \theta_2$ ($\theta_2 \le \theta \le \theta_3$). In particular cases, θ_1 and θ_3 can be respectively equal to 0 and π.

For a composite cone, eigensolutions (11.35) in each of the subdomains V_1 and V_2, must satisfy the equations of equilibrium (11.36), which will differ only in the values of the elastic material constants. In this case, one of the three variants of boundary conditions (11.37), (11.38) and (11.39) can be used for the surfaces $\theta = \theta_1$ ($\theta \ne 0$) and $\theta = \theta_3$ ($\theta \ne \pi$), while the condition on a contact surface is that of ideal bonding of layers

$$u_r^{(1)} = u_r^{(2)}, \quad u_\varphi^{(1)} = u_\varphi^{(2)}, \quad u_\theta^{(1)} = u_\theta^{(2)},$$
$$\sigma_\theta^{(1)} = \sigma_\theta^{(2)}, \quad \tau_{r\theta}^{(1)} = \tau_{r\theta}^{(2)}, \quad \tau_{\varphi\theta}^{(1)} = \tau_{\varphi\theta}^{(2)}, \tag{11.43}$$

or ideal sliding

$$u_\theta^{(1)} = u_\theta^{(2)}, \quad \sigma_\theta^{(1)} = \sigma_\theta^{(2)}, \quad \tau_{r\theta}^{(1)} = \tau_{r\theta}^{(2)} = \tau_{\varphi\theta}^{(1)} = \tau_{\varphi\theta}^{(2)} = 0. \tag{11.44}$$

We propose the following scheme of problem solution. Let us represent Eqs. (11.40) in a weak form [34], for which purpose we multiply them by the appropriate variations $\delta\xi_k(\theta,\varphi)$ and integrate over the region S cut by the cone from the sphere. As a result we get

$$\int_S \left[\sum_{k=1}^{3} L_k(\lambda, \xi_1, \xi_2, \xi_3)\, \delta\xi_k(\theta,\varphi) \right] dS = 0. \tag{11.45}$$

Equations (11.45) are solved using the finite element method (FEM). The finite-element implementation of these equations is a rather complicated procedure, since it requires the use of two-dimensional elements to ensure the continuity of the functions ξ_k, as well as the continuity of their first derivatives. Without going into details, we simply note that in FEM, there are no effective procedures for constructing such elements. In this regard, after performing identity transformations with the aim to reduce the order of derivatives of functions in the solutions of Eq. (11.45) and considering boundary conditions (11.42), we obtain the following equation

$$\begin{aligned}
&\iint_S \Big\{ \left[2(1-\nu)(k_1-2)\sin\theta\xi_1 + k_1(\cos\theta\xi_2 + \sin\theta\xi_{2\theta} + \xi_{3\varphi}) \right] \delta\xi_1 - \\
&\quad -(1-2\nu)(\sin\theta\xi_{1\theta}\,\delta\xi_{1\theta} + \frac{1}{\sin\theta}\xi_{1\varphi}\,\delta\xi_{1\varphi}) - \frac{2(1-\nu)}{\sin\theta}\xi_{3\varphi}\,\delta\xi_{3\varphi} + \\
&\quad + \left[(1-2\nu)k_1\sin\theta\xi_2 - \frac{2(1-\nu)}{\sin\theta}\xi_2 + k_3\sin\theta\xi_{1\theta} - (3-4\nu)\mathrm{ctg}\theta\xi_{3\varphi} \right] \delta\xi_2 - \\
&\quad -2(1-\nu)\sin\theta\xi_{2\theta}\,\delta\xi_{2\theta} - 2\nu\xi_{3\varphi}\,\delta\xi_{2\theta} - \\
&\quad -(1-2\nu)\left(\frac{1}{\sin\theta}\xi_{2\varphi}\,\delta\xi_{2\varphi} + \xi_{3\theta}\,\delta\xi_{2\varphi} \right) + \\
&\quad + \left[(1-2\nu)k_1\sin\theta\xi_3 - \frac{1-2\nu}{\sin\theta}\xi_3 + k_3\xi_{1\varphi} + (3-4\nu)\,\mathrm{ctg}\,\theta\xi_{2\varphi} \right] \delta\xi_3 - \\
&\quad -2\nu\xi_{2\theta}\,\delta\xi_{3\varphi} - (1-2\nu)\left(\sin\theta\xi_{3\theta}\,\delta\xi_{3\theta} + \xi_{2\varphi}\,\delta\xi_{3\theta} \right) \Big\}\, d\theta d\varphi + \\
&\quad + \int_l \{ (1-2\nu)(1-\lambda)\sin\theta\xi_2\,\delta\xi_1 - 2[(1+\nu\lambda)\sin\theta\xi_1 + \nu\cos\theta\xi_2]\delta\xi_2 + \\
&\quad + (1-2\nu)\cos\theta\xi_3\,\delta\xi_3 - (1-2\nu) \}\, dl = 0,
\end{aligned} \tag{11.46}$$

where l is the boundary of the surface S with prescribed stresses.

Reduction of the order of derivatives allows us to use such finite elements that ensure only the continuity of the functions ξ_k. In our simulation we used finite elements in the form of triangles and the Lagrangian linear polynomial approximation of the functions ξ_k.

In the numerical analysis of circular conical bodies with unmixed boundary conditions imposed on the lateral conical surfaces, the functions $\xi_k(\theta,\varphi)$ can be represented as a Fourier series in the circumferential coordinate φ

$$\begin{aligned} \xi_1 &= \sum_{n=0}^{\infty} \beta_1^{(n)}(\theta)\cos n\varphi, \\ \xi_2 &= \sum_{n=0}^{\infty} \beta_2^{(n)}(\theta)\cos n\varphi, \\ \xi_3 &= \sum_{n=0}^{\infty} \beta_3^{(n)}(\theta)\sin n\varphi. \end{aligned} \tag{11.47}$$

In view of expansion (11.47), Eqs. (11.45) and boundary conditions (11.41), (11.42) for each of the harmonics of the Fourier series can be written in the following form (dashed line indicates the derivative with respect to θ, the upper index (n) for $\beta_1, \beta_2, \beta_3$ is omitted):

$$\begin{aligned} \int_{\theta_1}^{\theta_2} \Big\{ \big[& 2(1-\nu)(k_1-2)\sin^2\theta\beta_1 + k_2(\cos\theta\sin\theta\beta_2 + \sin^2\theta\beta'_2 + n\sin\theta\beta_3) + \\ & + (1-2\nu)(\cos\theta\sin\theta\,\beta_1' + \sin^2\theta\beta_1'' - n^2\beta_1)\big]\,\delta\xi_1 + \big[(1-2\nu)k_1\sin^2\theta\beta_2 + \\ & + k_3\sin^2\theta\,\beta_1' - 2(1-\nu)\beta_2 - (1-2\nu)n^2\beta_2 + n\sin\theta\beta_3' - \\ & - (3-4\nu)n\cos\theta\beta_3 + 2(1-\nu)(\cos\theta\sin\theta\beta_2' + \sin^2\theta\beta_2'')\big]\,\delta\xi_2 + \\ & + \big[(1-2\nu)(k_1\sin^2\theta\beta_3 - \beta_3 + \cos\theta\sin\theta\,\beta_3' + \sin^2\theta\beta_3'') - k_3 n\sin\theta\beta_1 - \\ & - (3-4\nu)n\cos\theta\beta_2 - n\sin\theta\beta_2' - 2(1-\nu)n^2\beta_3\big]\,\delta\xi_3\Big\}\,d\theta = 0. \end{aligned} \tag{11.48}$$

$$\begin{aligned} M_1(\lambda,\beta_k) &\equiv \beta_1' + \beta_2(\lambda-1) = 0, \\ M_2(\lambda,\beta_k) &\equiv (1-\nu)\beta_2' + (1+\nu\lambda)\beta_1 + \nu\,\mathrm{ctg}\,\theta\beta_2 + \frac{\nu n}{\sin\theta}\beta_3 = 0, \\ M_3(\lambda,\beta_k) &\equiv \beta_3' + \frac{n}{\sin\theta}\beta_2 - \mathrm{ctg}\,\theta\,\beta_3 = 0. \end{aligned} \tag{11.49}$$

In the numerical implementation, the use of expansion (11.47) allows us to change from a two-dimensional problem to a set of separate one-dimensional problems for each of the harmonics of the Fourier series. In the finite element implementation of one-dimensional problems, in contrast to that of two-dimensional problems, the presence of well-tried finite elements ensures continuity of approximating functions and their first derivatives between two adjacent elements. It means that in this case we can directly carry out the finite element implementation of Eqs. (11.48). As finite elements, we used one-dimensional two-node elements, in which the functions $\beta_i^{(n)}(\theta)$ are approximated with a cubic polynomial defined by the values of the function and its derivatives $d\beta_i^{(n)}/d\theta$ at the ends of the segment (one-dimensional element).

As in a two-dimensional version, we can employ the procedure of reducing the order of derivatives in Eq. (11.48). Then, in the case of applying the finite element method of solution to these equations, it becomes possible to use one-dimensional elements ensuring continuity of only approximated functions, in particular, one-dimensional two-node elements with linear approximation of functions $\beta_i^{(n)}(\theta)$.

The application of the Bubnov procedure together with the finite element method reduces the formulated problem to a search for eigenvalues (EV) and eigenvectors of an algebraic asymmetric band matrix. To find complex eigenvalues, the obtained algebraic problem is solved using the algorithm based on the application of the Muller method and the argument principle [17], which allowed us to obtain acceptable numerical results.

The reliability and efficiency of the proposed method and the algorithm for its numerical implementation can be substantiated by the results of two numerical experiments. The first experiment is designed to realize the possibility of comparing the numerical and analytical results for a homogeneous continuous circular cone ($0 \leq r \leq \infty$, $0 \leq \varphi \leq 2\pi$, $0 \leq \theta \leq \theta_2$) [15]. In a two-dimensional variant with the number of nodal variables equal to $\sim 10^3$, the difference between the numerical and analytical results is less than one percent. The second computational experiment is based on the analysis of the convergence of the numerical method depending on the degree of discretization of the computational domain. As an example, Fig. 11.7a shows a numerical solution (solid curve) depending on the number of nodal variables N and analytical results (dashed curve) at $\theta_2 = 2\pi/3$, $\nu = 0.3$. The results of such experiments demonstrate not only the convergence of the numerical procedure, but also make it possible to choose a variant of discretization of the computational domain, which can provide acceptable accuracy.

Let us consider the results of solving a number of new problems. Figure 11.7b presents the eigenvalues calculated for a solid circular cone ($\nu = 0.3$) at boundary conditions (11.39) corresponding to the ideal sliding conditions. Figure 11.7c displays the eigenvalues for one of the variants of a continuous circular cone ($\theta_2 = 2\pi/3$, $\nu = 0.3$) at mixed boundary conditions prescribed on the lateral surface: zero displacements at and zero stresses at $\varphi_1 \leq \varphi \leq 2\pi$. It should be noted that in this problem, the representation of the desired solution as a Fourier series in the angular coordinate φ is not allowed. Hereinafter, the solid curve corresponds to real eigenvalues, while the dashed curve corresponds to the complex eigenvalues.

Calculations were performed for a composite cone which allowed us to evaluate the effect of ratios of mechanical characteristic on the stress singularity exponents. In Fig. 11.8, for the composite cone under boundary conditions (11.43) and $\theta_1 = 0$, $\theta_2 = \pi/3$, $\theta_3 = 2\pi/3$, $\nu_1 = \nu_2 = 0.3$ the values of $\mathrm{Re}\lambda_\mathrm{k} < 1$ are plotted against the ratio G_1/G_2.

The method under consideration allows us to obtain numerical results for different cone shapes, including a cone whose base is an ellipse. The geometry of the boundary of the surface (11.46), which is cut by a cone from a sphere, is defined by

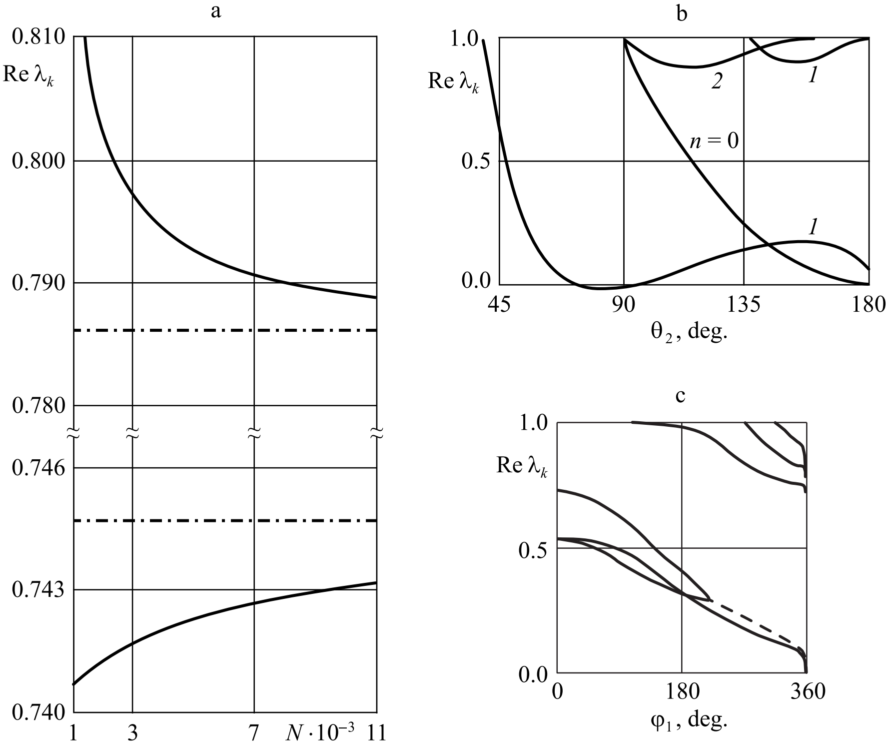

Fig. 11.7 Dependence of Reλ_k on the value of N (a). Dependences of Reλ_k on the angle θ_2 (b) and on the angle φ_1 (c)

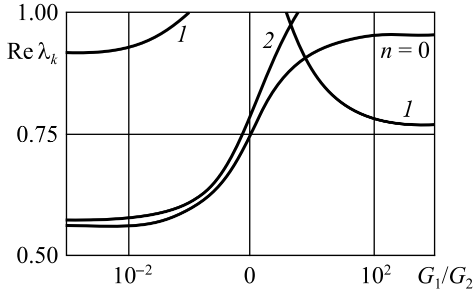

Fig. 11.8 Dependence of Reλ_k on the ratio G_1/G_2

the relation

$$\mathrm{tg}\theta = \mathrm{tg}\theta_2 \left(\frac{1}{\left(\cos^2\varphi + æ^{-2}\sin^2\varphi\right)^{-/2}} \right), \qquad æ = \frac{\mathrm{a}}{\mathrm{b}}. \tag{11.50}$$

Here a and b are the semi-axes of the ellipse, $2\theta_2$ is the vertex angle of the cone in the plane passing through the cone vertex and the semi-axis a. Figure 11.9 shows

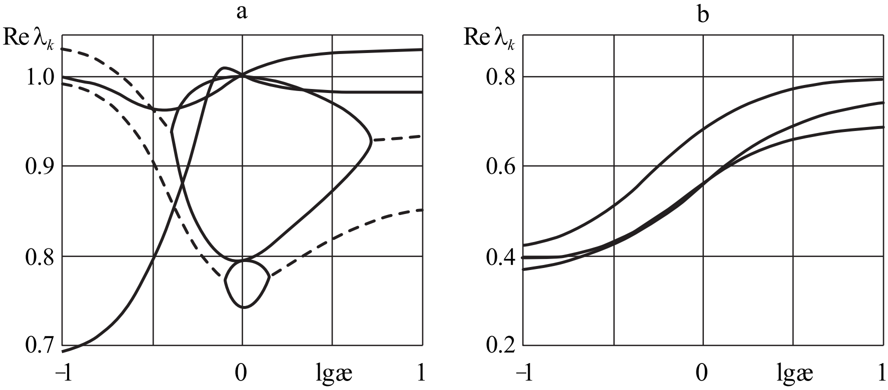

Fig. 11.9 Dependence of Reλ_k on the value of æ at zero stress (a) and at zero displacement (b)

the results of calculations of eigenvalues at zero stress (a) and at zero displacement (b) specified on the lateral surface of the cone.

The proposed method has proved to be effective in calculating all eigenvalues of interest. Furthermore, within the error of the numerical method, it allows one to calculate multiple eigenvalues. For example, in [15] analytical results on the multiplicity of the eigenvalue $\lambda = 1$ were presented. In particular, at $\theta_2 = \pi/2$ the multiplicity is found to be 6 and at $\theta_2 = \pi$ the multiplicity is 9. The method under consideration can be used to find all multiple eigenvalues within the accuracy of the third place with the number of finite elements being equal to about three thousand.

11.4 Finite Element Analysis of Stress Singularity in Three-dimensional Problems of Elasticity Theory

To determine the power law relationship of stresses in the vicinity of singular points, a numerical technique [29] is proposed. It is based on the statement that the stress distribution along the radial line, originating from a singular point, can be expressed as [4, 35]

$$\sigma = A_1 r^{\lambda-1} + O(r^{\lambda}), \tag{11.51}$$

where r is the distance from the singular point, A_1 is some constant, λ is the parameter, characterizing the degree of stress singularity, and $O(r^{\lambda})$ represents all terms of the order r^{λ} and higher. For small distances r, the singular term dominates and equation (11.51) can be approximated by

$$\sigma \simeq A_1 r^{\lambda-1},$$

or

$$\log\sigma = \log A_1 + (\lambda-1)\log r, \tag{11.52}$$

where λ is the smallest eigenvalue [4]. The parameter λ is determined using the FEM procedure with finite element meshes refined towards the singular points (Fig. 11.10). To establish the relationship (11.52) via numerical experiments, it is necessary to find the discretization, such that in the vicinity of a singular point at a number of nodal points on the radial line originating from the singular point the following relations will be fulfilled with sufficient accuracy:

$$\lambda - 1 \approx \frac{\log\left(\frac{\sigma_1}{\sigma_2}\right)}{\log\left(\frac{r_1}{r_2}\right)} \approx \frac{\log\left(\frac{\sigma_2}{\sigma_3}\right)}{\log\left(\frac{r_2}{r_3}\right)} \approx \ldots \approx \frac{\log\left(\frac{\sigma_{n-1}}{\sigma_n}\right)}{\log\left(\frac{r_{n-1}}{r_n}\right)}, \qquad (11.53)$$

where $r_1, r_2, \ldots, r_n$ are the distances from the singular point, $\sigma_1, \sigma_2, \ldots, \sigma_n$ are stresses at the corresponding nodal points $r_1, r_2, \ldots, r_n$, respectively. λ is the required stress singularity exponent. The derivation of this relationship makes it possible to calculate the value of λ, which determines the stress behavior (including that of stress singularity) in the vicinity of a singular point.

The algorithm is tested by solving two- and three-dimensional problems of elasticity theory and comparing the stress singularity exponents found by the proposed numerical algorithm with those obtained from the known analytical and numerical solutions. As two-dimensional problems, we considered a plate with notches (Fig. 11.11a), a plate with a fixed edge (Fig. 11.11b), and a composite plate (Fig. 11.11c), which contained singular points associated, respectively, with breaking of surface smoothness, a change in the type of boundary conditions, and a contact of dissimilar materials. For all problems, the obtained numerical results agree with the analytical results up to the third decimal place.

The proposed numerical algorithm for computing the stress singularity exponents in the vicinity of singular points is of considerable independent significance for problems, which cannot be solved analytically in the vicinity of singular points. To problem of crack propagation, whose front is perpendicular to the surface xOy of an

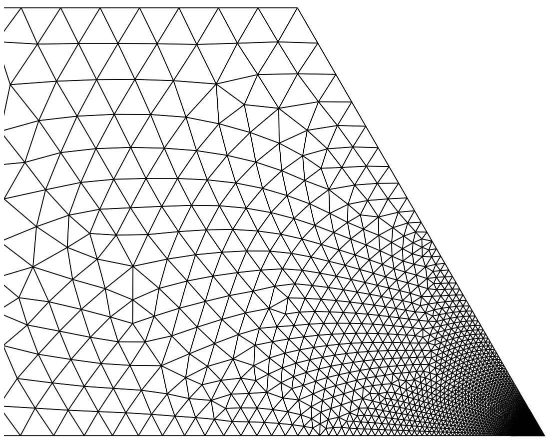

Fig. 11.10 The example of finite-element mesh with gradual refinement near singular point

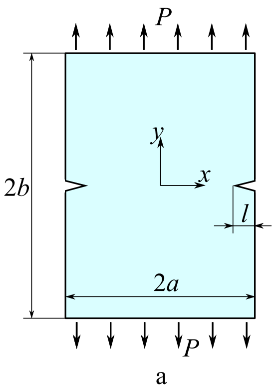

Fig. 11.11 Plate with V-notches on lateral edges (a); plate with a fixed edge (b); composite plate (c)

elastic half-space (Fig. 11.12a). The stress singularity exponent is evaluated at the tip of the crack with coordinates $x = y = z = 0$. For this problem, work [23] presents the results of numerical calculation of stress singularity exponents for an isotropic material ($\nu = 0.3$) and an orthotropic material, the elastic characteristics of which are summarized in Table 11.1.

As a computational scheme for this problem, we use a cube (Fig. 11.12b). The conditions of opening mode (the mode I) are simulated by the normal displacements applied parallel to the xOz-plane, and the conditions of sliding mode (the mode II) are simulated by the tangential displacements applied parallel to the x-axis and in the opposite directions.

Table 11.2 presents the values of stress singularity exponents for a crack tip under loads of mode I and II obtained in [23] and calculated with the proposed numerical

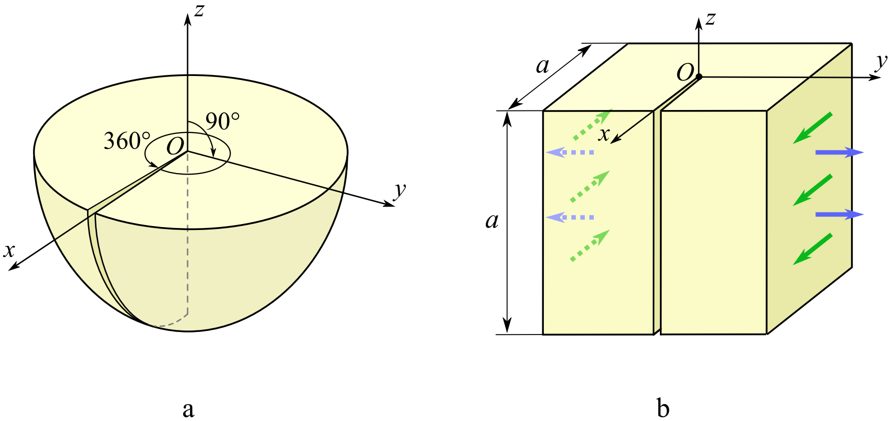

Fig. 11.12 Crack, the front of which is perpendicular to the surface of an elastic half-space (a); its computational scheme (b)

Table 11.1 Elastic characteristics of carbon fiber reinforced plastic [23]

Material	E_i, GPa	G_{ij}, GPa	ν_{ij}
	$E_x = 130.3$	$G_{xy} = 4.502$	$\nu_{xy} = 0.33$
Carbon fiber reinforced plastic	$E_y = 9.377$	$G_{xz} = 4.502$	$\nu_{xz} = 0.33$
	$E_z = 9.377$	$G_{yz} = 2.865$	$\nu_{yz} = 0.33$

Table 11.2 Comparison between stress singularity exponents calculated by formula (11.53) and obtained in [23] for a crack whose front is perpendicular to the surface of an elastic half-space (three-dimensional problem)

	Isotropic ($\nu = 0.3$)		Anisotropic (Table 11.1)	
	λ_1 (mode II)	λ_2 (mode I)	λ_1 (mode II)	λ_2 (mode I)
Numerical algorithm	0.40	0.55	0.46	0.52
Numerical result from [23]	0.3929	0.5483	0.4543	0.5227

algorithm, which uses the finite element method to determine the stress asymptotics based on relations (11.53). In this case, the difference between the stress singularity exponents calculated by formula (11.53) and those presented in [23] is less than 1.8%.

Hence, the effectiveness and high accuracy of the proposed numerical algorithm for calculating the stress singularity exponents in the vicinity of singular points for homogeneous and piecewise homogeneous bodies, including those with anisotropic properties have been substantiated by the results of solution of two- and three-dimensional problems of elasticity theory.

11.5 Conclusion

The analytical method for constructing eigenvalues for circular cones has been considered. The relations developed in this study can be used to construct solutions, and estimate the character of stress singularity for different variants of conical bodies (solid, hollow, composite cones) under different types of boundary conditions set on the lateral surfaces and contact surfaces of different materials. Numerical results have been presented on the nature of stress singularity at the vertex of a solid cone under boundary conditions specified in terms of displacements, stresses, mixed type boundary conditions and at the vertex of a hollow cone under different variants of boundary conditions specified on the lateral surfaces. A numerical algorithm for evaluating the nature of stress singularity in the vicinity of singular points of elastic bodies has been considered. It is based on the derivation of a power law relationship for stresses from the numerically determined stress-strain state in the vicinity of a singular point. The efficiency and high accuracy of the proposed numerical algorithm for calculating stress singularity exponents in the vicinity of singular points for homogeneous and piecewise homogeneous bodies, including those with anisotropic properties, have been demonstrated.

Acknowledgements Sections 11.2 and 11.3 were performed within the state assignment of ICMM UB RAS (topic No. AAAA-A19-19012290100-8). Section 11.4 was funded by RFBR and Perm Territory (project No. 20-41-596007).

References

1. T. Apel, V. Mehrmann, and D. Watkins. Structured eigenvalue methods for the computation of corner singularities in 3d anisotropic elastic structures. *Computer Methods in Applied Mechanics and Engineering*, 191(39):4459–4473, 2002.
2. V.A. Babeshko, E.V. Glushkov, N.V. Glushkova, O.N. Lapina. Stress singularity in the vicinity of the vertex of an elastic trihedron. *Dokl. Akad. Nauk SSSR*, 318(5):1113–1116, 1991.
3. Z.P. Bazant, L.M. Keer. Singularities of elastic stresses and harmonic functions at conical notches and inclusions. *International Journal of Solids and Structures*, 10(9):957–965, 1974.
4. E.B. Becker, R.S. Dunham, and M. Stern. Some stress intensity calculations using finite elements. in V.A. Pulmans, A.P. Kabaila, editors, *Finite element methods in engineering : proceedings of the 1974 International Conference on Finite Element Methods in Engineering*, pages 117–138, Kensington, May 1974. the School of Civil Engineering, the University of New South Wales, Unisearch Ltd.
5. A. Carpinteri, M. Paggi. Asymptotic analysis in linear elasticity: From the pioneering studies by Wieghardt and Irwin until today. *Engineering Fracture Mechanics*, 76(12):1771–1784, 2009.
6. A. Dimitrov, H. Andrä, E. Schnack. Singularities near three-dimensional corners in composite laminates. *International Journal of Fracture*, 115(4):361–375, 2002.
7. J.W. Eischen. Fracture of nonhomogeneous materials. *International Journal of Fracture*, 34(1):3–22, 1987.
8. A.Yu. Fedorov, V.P. Matveenko. Investigation of stress behavior in the vicinity of singular points of elastic bodies made of functionally graded materials. *Journal of Applied Mechanics*, 85(6):061008, apr 2018.
9. C.S. Huang, A.W. Leissa. Stress singularities in bimaterial bodies of revolution. *Composite Structures*, 82(4):488–498, 2008.
10. E. Kamke. *Differentialgleichungen: Lösungsmethoden und Lösungen*. Vieweg+Teubner Verlag Wiesbaden, Leipzig, 1977.
11. H. Koguchi. Stress singularity analysis in three-dimensional bonded structure. *International Journal of Solids and Structures*, 34:461–480, 1997.
12. V.A. Kondrat'ev. Boundary value problems for elliptic equations in domains with conical or angular points. *Transactions of the Moscow Mathematical Society*, 16:227–313, 1967.
13. T.O. Korepanova, V.P. Matveenko, N.V. Sevodina. Numerical analysis of stress singularity at singular points of three-dimensional elastic bodies. *Acta Mechanica*, 224(9):2045–2063, 2010.

14. T.O. Korepanova, V.P. Matveenko, I.N. Shardakov. Analytical constructions of eigensolutions for isotropic conical bodies and their applications for estimating stress singularity. *Doklady Physics*, 59(7):335–340, 2014.
15. V.A. Kozlov, V. Maz'ya, and J.S. Rossmann. *Spectral Problems Associated with Corner Singularities of Solutions to Elliptic Equations*. American Mathematical Society, Rhode Island, 2001.
16. V.P. Matveenko, T.O. Nakaryakova, N.V. Sevodina, I.N. Shardakov. Investigation of singularity of stresses at the apex of a cone with an elliptic base. *Doklady Physics*, 51(11):630–633, 2006.
17. V.P. Matveenko, M.A. Sevodin, N.V. Sevodina. Applications of Muller's method and the argument principle to eigenvalue problems in solid mechanics. *Computational Continuum Mechanics*, 7(3):331–336, 2014.
18. N.M. Matveev. *Integration Techniques of Ordinary Differential Equations*. Higher School, Moscow, 1967.
19. V.P. Matveyenko, T.O. Nakaryakova, N.V. Sevodina, I.N. Shardakov. Stress singularity at the vertex of homogeneous and composite cones for different boundary conditions. *Journal of Applied Mathematics and Mechanics*, 72(3):331–337, 2008.
20. S.E. Mikhailov. Stress singularity in the vicinity of an angle edge in an anisotropic composite and some applications to fibrous composites. *Izv. Akad. Nauk SSSR, Mekh. Tverd. Tela*, (5):103–110, 1979.
21. N.F. Morozov. Brittle fracture problems and their solution using elasticity methods. In *Mechanics and Progress in Science and Engineering, Vol. 3: Solid Mechanics [in Russ.]*, pages 54–63. Nauka, Moscow, 1988.
22. N.F. Morozov, B.N. Semenov. Using the Novozhilov criterion of brittle fracture to determine fracture loads for V-shaped notches in complex stressed states. *Izv. Akad. Nauk SSSR, Mekh. Tverd. Tela*, (1):122–126, 1986.
23. S.S. Pageau, S.B. Biggers. Finite element evaluation of free-edge singular stress fields in anisotropic materials. *International Journal for Numerical Methods in Engineering*, 38(13):2225–2239, 1995.
24. S.S. Pageau, S.B. Biggers. A finite element approach to three-dimensional singular stress states in anisotropic multi-material wedges and junctions. *International Journal of Solids and Structures*, 33(1):33–47, jan 1996.
25. M. Paggi, A. Carpinteri. On the stress singularities at multimaterial interfaces and related analogies with fluid dynamics and diffusion. *Applied Mechanics Reviews*, 61(2):020801, 2008.
26. K.S. Parihar, L.M. Keer. Elastic stress singularities at conical inclusions. *International Journal of Solids and Structures*, 14(4):261–263, 1978.
27. C.R. Picu, V. Gupta. Three-dimensional stress singularities at the tip of a grain triple junction line intersecting the free surface. *Journal of the Mechanics and Physics of Solids*, 45(9):1495–1520, 1997.
28. L.P. Pook. A 50-year retrospective review of three-dimensional effects at cracks and sharp notches. *Fatigue & Fracture of Engineering Materials & Structures*, 36(8):699–723, 2013.
29. I.S. Raju, J.H. Crews. Interlaminar stress singularities at a straight free edge in composite laminates. *Computers & Structures*, 14(1):21–28, 1981.
30. M.P. Savruk, S. Shkarayev. Stress singularities for three-dimensional corners using the boundary integral equation method. *Theoretical and Applied Fracture Mechanics*, 36:263–275, 2001.
31. G.B. Sinclair. Stress singularities in classical elasticity – I: Removal, interpretation, and analysis. *Applied Mechanics Reviews*, 57(4):251–297, 2004.
32. G.B. Sinclair. Stress singularities in classical elasticity – II: Asymptotic identification. *Applied Mechanics Reviews*, 57(5):385–439, 2004.
33. N. Somaratna and T.C.T. Ting. Three-dimensional stress singularities at conical notches and inclusions in transversely isotropic materials. *Journal of Applied Mechanics*, 53(1):89–96, 1986.
34. G.Strang and G.J. Fix. *An Analysis of the Finite Element Method*. Prentice-Hall, Inc., Englewood, N.J., 1973.

35. M.L. Williams. Stress singularities resulting from various boundary conditions in angular corners of plates in extension. *Journal Applied Mechanics*, 19(4):526–528, 1952.